Comparison between the Optical Performance of Photonic Bandgap and Antiresonant Hollow Core Fibers after Long-Term Exposure to the Atmosphere

Shuichiro Rikimi[1*], Yong Chen[1,2], Thomas D Bradley[1], Ian A Davidson[1], Hesham Sakr[1], Austin A Taranta[1], Kerrianne Harrington[1], Francesco Poletti[1], Marco N Petrovich[1,2], David J Richardson[1,2], Natalie V Wheeler[1]

[1]*Optoelectronics Research Centre, University of Southampton, SO17 1BJ, UK;*

[2]*Lumenisity Ltd., Unit 7, The Quadrangle, Romsey, SO51 9DL, UK; *sr1y15@soton.ac.uk*

Abstract: We measure the changes in transmission properties of two different hollow core fiber types exposed to standard atmosphere over nearly one year. No degradation of transmitted power is observed for the hollow-core NANF studied.

1. Introduction

Hollow core fibers (HCFs) are a specialty optical fiber, with optical properties controlled by a microstructured cladding, consisting of carefully arranged air holes and thin glass membranes, which enables light to propagate with low loss in air. State-of-the-art Nested Antiresonant Nodeless Fibers (NANFs) have demonstrated very low loss in both the main telecommunication bands and visible wavelength regions [1,2] and also offer additional advantages, such as high polarization purity [3] and very low backscattering [4]. Recently the first successful field installation of cabled NANF for data transmission was reported [5] and increasing demand for HCFs for various applications is expected in the near future. Now, one of the critical needs to enable deployment in practical systems is in ensuring reliability of the optical performance of HCFs, of which little is currently known. While HCFs are immune from material degradations that affect the solid glass core, they might suffer from different degradation mechanisms linked to the unique geometrical features of the microstructured cladding and the presence of gas species inside the hollow channels which run along the entire fiber length. For data transmission applications, HCFs are spliced to conventional solid fibers; this provides a hermetic seal and prohibits atmospheric ingress into the fiber over time, and we have previously reported that in this form, the transmission of the HCF (made of Heraeus F300 glass) did not degrade over ~20 months [6] (and as of now ~3 years). However, some work has also been reported highlighting the affinity of water vapor with the internal surfaces in an HCF, demonstrating growth of surface OH absorption features in an HCF open to continuous exposure to a humidity-containing atmosphere [7]. Furthermore, we have recently shown that, immediately after fabrication, HCFs have an internal pressure substantially below atmospheric pressure, and such pressure difference can accelerate the ingress of water vapor and other atmospheric gas species into an HCF [8]. Although the overlap of the light guided in an HCF with the cladding structure is extremely low [9,10] and could render these fibers relatively insensitive to surface changes, the impact of humidity on the broadband transmission of an HCF has not yet been investigated, and this is likely to prove an important aspect for consideration of the long-term optical performance or in the event of a fiber break during or after deployment.

Therefore, we devote the present study to the impact of humidity-containing standard atmosphere on the optical performance of HCFs. While in a scenario such as a fiber break, the HCF may only be open to atmosphere for a short time period, here we kept single end of each tested HCF sample open to a humidity-containing atmosphere continuously for nearly 1 year, in order to enhance and potentially promote possible degradation. Furthermore, two different fiber designs were studied; 5-nested tubes NANF (5T-NANF) and 7-cell HC-Photonic Band-Gap Fiber (7C-PBGF). The NANF was selected as it is similar to recent state-of-the-art HCFs [1] while the 7C-PBGF structure was specifically selected to enhance sensitivity to surface conditions of the hollow core, as this fiber design has a relatively higher overlap between the guided light and the cladding membranes. Our results show that, while a substantial reduction in the optical performance was recorded for the 7C-PBGF, the transmission of the 5T-NANF did not show any reduction due to ageing in the measurement environment over >300 days.

2. Fiber characteristics, preparation and experimental procedures

Scanning electron microscope images of the two types of HCFs used for this work are presented in Fig. 1(a). The 5T-NANF has a 32.7 μm diameter core; this antiresonant fiber design was selected due to its similarity to the record low loss 5T-NANF design (0.22 dB/km at 1625 nm) [1]. The 7C-PBGF, which has a 24.4 μm diameter core, was selected because it has an overlap between the guided light and the cladding ~2 orders of magnitude higher than the 5T-NANF design, although it is still only ~1 % [9]. This makes it an interesting structure to use to detect any changes affecting the inner silica core wall. The HCFs were fabricated using a standard stack and draw technique [9]. Here, two raw glass materials were used to fabricate the HCFs [11]. The 5T-NANF was made from Heraeus F300 containing 800-2000 ppm of chlorine, which is a standard material for optical fiber fabrication, while the 7C-PBGF was fabricated using a cane made from Heraeus F320-08 inserted into a F300 jacket tube. F320-08 contains ~3000 ppm of fluorine and reduced chlorine content (200-300 ppm). F320-08 was selected to reduce a previously observed and undesirable contribution from chlorine in the glass material, whereby ammonium chloride forms on the end-face of a cleaved HCF [12]. The results of cut-back loss measurements on both fibers studied are shown in Fig. 1(a). The losses at 1550 nm of the 5T-NANF and the 7C-PBGF are 1.72 ± 0.11 dB/km and 11.2 ± 1.17 dB/km, respectively. Features in the attenuation between ~1340-1500 nm observed from the 5T-NANF can be attributed to water vapor which was present inside the hollow core, while those observed from the 7C-PBGF combine water vapor and surface OH absorption [7,13], which highlights the higher overlap of the guided light with the glass surfaces in the 7C-PBGF.

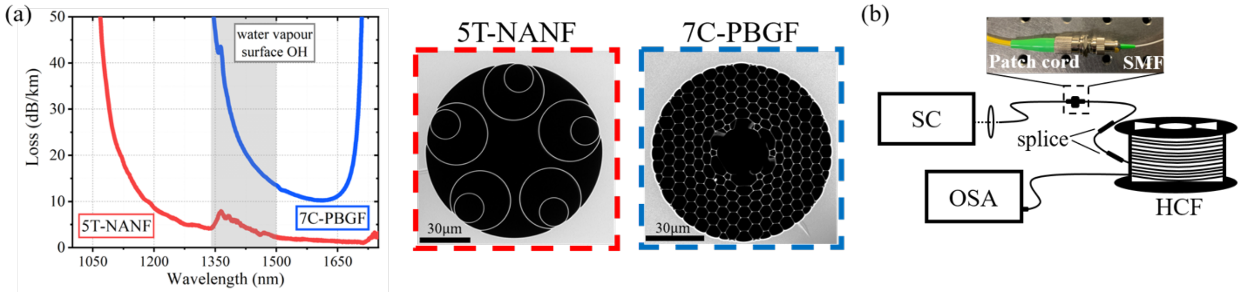

Fig. 1. (a) Loss and SEM images of the 5T-NANF (yellow) and the 7C-PBGF (blue). (b) The experimental setup. The spliced sections were actually fixed onto the bobbins but are shown separately here for clarity. The patch cord was disconnected after each measurement.

Following the method described in [8], the ends of these HCFs were sealed immediately after fabrication to isolate the internal conditions of the fibers from the atmosphere and to try to ensure consistent initial conditions between the different fiber samples. After characterization, 155 m of the 5T-NANF and 150 m of the 7C-PBGF were rewound on 31.5 cm diameter bobbins and one end of each fiber was spliced to a solid fiber pigtail to maintain consistent coupling efficiency for repeated transmission measurements. This pigtail consisted of an all-solid large mode area fiber spliced to a FC/APC connectorized single mode fiber (SMF) pigtail. The experimental setup for transmission measurements is described in Fig. 1(b). A collimated beam from a supercontinuum laser (Fianium SC400) was lens-coupled into a short FC/APC-connectorized SMF patch cord, which was then connected to the spliced HCF assembly via an FC/APC mating adapter. The other (open) end of the HCF assembly was connected to an optical spectrum analyzer (OSA AQ6315A) using a bare-fiber adapter. The open fiber end was freshly cleaved just before beginning each measurement and the transmission spectrum was sequentially recorded using the OSA for resolutions of 10 nm and 0.05 nm. Between measurements, the open fiber end remained open to the lab atmosphere (40% RH and 22°C controlled humidity and temperature, respectively).

3. Experimental results and discussion

The evolution of the transmission spectra of the two HCFs are shown in Fig. 2(a) and (b). Two trends from this data are immediately clear. Firstly, the 7C-PBGF transmission significantly degrades over time; the attenuation not only inside but also outside the water vapor and the surface OH absorption region significantly increases. On the other hand, the 5T-NANF transmission remains consistent over the ~10 months over which measurements were taken. The transmission consistency of the HCFs was evaluated by comparing the change in the transmitted power over time with that measured immediately after opening the fiber end (e.g. Day0-Day1). The consistency of the 5T-NANF transmission is highlighted in Fig. 2(c) which shows the fiber transmission over time at two relevant wavelengths (1300 nm – away from water vapor and OH absorption; 1550 nm – telecoms); no degradation of the optical performance was observed even after 304 days of atmospheric exposure. Further analysis of the 7C-PBGF transmission changes is highlighted in Fig. 2(d)-(f). In Fig. 2(d), the evolution of the transmitted power through the 7C-PBGF for three wavelengths is plotted with respect to time, showing that the transmitted power started to reduce after opening the sealed fiber end, continued to decrease at a decreasing rate until ~50 days and then finally plateaued. This suggests that ingress of the atmosphere into the pristine fiber is responsible for the loss degradation.

The transmission loss of the 7C-PBGF, measured between 1340 and 1500 nm with the OSA (0.05 nm resolution), is shown in Fig. 2(e). In addition to the narrow absorption features due to water vapor inside the hollow core, a more broadband, continuous background feature clearly increases in magnitude over time. This background includes the isolated surface silanol (SiOH) at 1364 nm and the broad absorption originating from the hydrogen-bonded SiOH/water groups [13,14]. Note that the surface OH features were not detected from the 5T-NANF and this can be attributed to the negligible interaction of light propagating in the NANF hollow core with the core surface. Fig. 2(f) shows the evolution of the isolated surface OH absorption strength. The absorption increased after opening the fiber end over the same time scale as the broadband reduction in the transmitted power. As seen in Fig. 2(d), the ageing of the 7C-PBGF has a clear wavelength dependence (irrespective of the OH absorption features); the degradation was more severe at shorter wavelengths. Correlating the observation that the ageing character is highly-dependent on the nature of the microstructure and that the loss increase has a strong wavelength dependence with the growth of the surface OH concentration, we believe that the loss increase is highly likely due to an additional scattering source by multilayers of the water/OH groups on the silica hollow core surface due to subsequent adsorption of the atmospheric water vapor [6,15]. The fraction of power on the core surface in the NANF structure is only ~30-50 ppm [10], too low to cause additional scattering, despite the OH-roughened surfaces. It is worth noting that here the performance degradation was observed from the 7C-PBGF made from F320 glass; ongoing work aims to establish whether the fluorine content might have an impact on the observed ageing.

Although the exposure of HCF inner surfaces to atmospheric moisture presents a potential hazard for reliable optical performance, by reducing the interaction area of light with the inner core surfaces, antiresonant structures possess an inherent advantage with respect to changes in surface scattering induced by aging. Splicing both HCF ends with solid fibers to make a hermetically sealed HCF cell [6] has previously been shown to maintain the transmission of an HCF without any degradation and we have again confirmed the effectiveness of this in preventing transmission degradation using the 7C-PBGF used in this paper; the results (not shown here) show the transmission of the 7C-PBGF when hermetically spliced has not changed over ~3 months and measurements are ongoing.

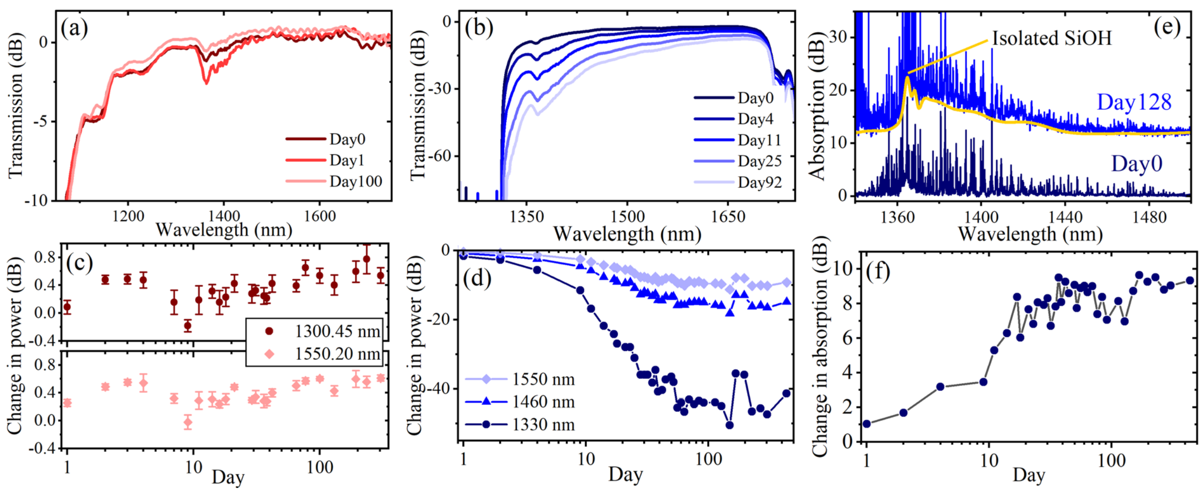

Fig. 2. The transmission spectrum of (a) the 5T-NANF and (b) the 7C-PBGF at selected days after opening the fiber end. Change in the transmitted power of (c) the 5T-NANF and (d) the 7C-PBGF for selected wavelengths. The error bars here represent experimental uncertainty due to the variable connections and the different cleaves for different measurements. (e) The surface OH related absorption measured from the 7C-PBGF on Day0 and Day128. 12 dB of an offset was added to the Day 128. (f) Change in the isolated SiOH absorption in the 7C-PBGF.

4. Conclusion

While more comprehensive aging tests on NANFs will need to be conducted in due time, this study presents a first attempt to try to understand the influence of humidity-containing air on the broadband optical reliability of HCFs. The transmitted spectrum of low loss 5T-NANF did not show noticeable degradation after atmospheric exposure. In contrast, significant, progressive loss degradation was observed in a 7C-PBGF and this was highly likely due to additional surface scattering by adsorption of atmospheric water vapor on the core surface. The use of a NANF design providing very small sensitivity to surface conditions and/or hermetically splicing with solid fibers to isolate the internal surfaces from atmospheric humidity can be effective means to suppress the ageing. These findings are an important initial step toward further reliability study of HCF technologies.

This project gratefully acknowledges funding from Lumenisity Ltd, EPSRC Programme grant “AirGuide Photonics” (EP/P030181/1), the EPSRC National Hub in High Value Manufacturing (EP/N00762X/1), ERC project LightPipe (grant agreement n° 682724) and the Royal Society.

[1] H. Sakr et al, in Proc. OFC 2021, paper F3A.4.
[2] H. Sakr et al, *Nat. Commun.*, 11, 6030, 2020.
[3] A. Taranta et al, *Nat. Photonics*, 14, 504-510, 2020.
[4] V. Michaud-Belleau et al, *Optica*, 8, 216-219, 2021.
[5] euNetworks, Media and press releases, 14th Apr. 2021.
[6] S. Rikimi et al, in Proc. WSOF2019, paper 112061U.
[7] I. G. Sanchez, J. C. Knight, *J.Light.Tech.*, 30,3597-3602, 2012.
[8] S. Rikimi et al, in Proc. AP2020, paper SoW1H.4.
[9] F. Poletti et al, *Nanophotonics*, 2, 315-340, 2013.
[10] F. Poletti, *Opt. Express*, 22, 23807–23828, 2014.
[11] Heraeus, Data sheet – High purity fused silica tubes, 2020.
[12] S. Rikimi et al, in Proc. CLEO 2020, paper SF2P.4.
[13] R. T. Bise and D. J. Trevor, in Proc. OFC 2004, paper WI4.
[14] R. S. McDonald, *J. Phys. Chem.*, 62, 1168-1178, 1958.
[15] L. T. Zhuravlev, *Colloids and Surfaces*, 173, 1-38, 2000.